

## Coverage dependence of the dynamics of ethylene adsorption on Ag(210)

This article has been downloaded from IOPscience. Please scroll down to see the full text article.

2004 J. Phys.: Condens. Matter 16 S2929

(<http://iopscience.iop.org/0953-8984/16/29/008>)

View [the table of contents for this issue](#), or go to the [journal homepage](#) for more

Download details:

IP Address: 129.252.86.83

The article was downloaded on 27/05/2010 at 16:07

Please note that [terms and conditions apply](#).

# Coverage dependence of the dynamics of ethylene adsorption on Ag(210)

L Vattuone, L Savio and M Rocca

Istituto Nazionale di Fisica della Materia, Unità di Genova, IMEM-CNR, Sezione di Genova, and Dipartimento di Fisica, Via Dodecaneso 33, 16146 Genova, Italy

Received 4 May 2004

Published 9 July 2004

Online at [stacks.iop.org/JPhysCM/16/S2929](http://stacks.iop.org/JPhysCM/16/S2929)

doi:10.1088/0953-8984/16/29/008

## Abstract

The sticking probability of C<sub>2</sub>H<sub>4</sub> on Ag(210) is studied by the molecular beam technique and by high resolution electron energy loss spectroscopy. At a crystal temperature of 110 K, adsorption occurs initially into a stable,  $\pi$ -bonded, state. At larger coverage a metastable state is populated, too. The sticking probability,  $S$ , decreases with increasing translational energy indicating non-activated adsorption. At low coverage and for impact angles from  $-60^\circ$  to  $+60^\circ$ ,  $S$  is angle independent, decreasing only as soon as the (100) nanofacets start to be shadowed. At higher coverage, in contrast,  $S$  depends on the impact angle, decreasing markedly for grazing incidence onto the (100) nanoterraces. The saturation coverage corresponds to quarter occupancy of the available step sites.

## 1. Introduction

Adsorption constitutes a fundamental step in catalytic reactions, and it has therefore been thoroughly investigated by surface scientists for nearly perfect low Miller index surfaces in controlled ultra-high vacuum (UHV) conditions. Industrial reactions occur, however, at high pressure and on finely dispersed powders, resulting in two serious limits of the surface science approach, known as *structure* and *pressure* gaps. The former arises from the atomic termination rich in defects, such as steps, kinks, adatoms, etc, present at the surface of the active grains. The latter is due to the difference of 13 orders of magnitude between the pressure present in industrial reactors and that of the UHV chambers used for surface science experiments.

In order to bridge the pressure gap one can take advantage of molecular beam techniques, allowing one to dose reactants at hyperthermal energies and thus sampling the effect of the high energy tail of the Maxwell distribution, which may determine the reaction rate for activated adsorption systems. The structure gap can be tackled, on the other hand, by studying high Miller index surfaces, exhibiting a well defined majority defect (steps, isolated kinks, etc),

depending on the indices of the surface. In this way it is possible to investigate the role of a certain, well defined defect at the atomic level.

Hydrocarbon chemistry at surfaces is the subject of a vast literature [1, 2]. Ethylene adsorption at Ag surfaces [3, 4] is particularly important for the understanding of the so-far unsolved ethylene epoxidation reaction [5–8] for which surface defects might play a pivotal role. This paper follows our previous investigations of  $C_2H_4$  adsorption on Ag(100) and Ag(410) [9–15]. In these experiments we demonstrated that physisorbed and  $\pi$ -bonded states exist on Ag(100) and are characterized by a different adsorption energy [9] and by a different C 1s photoemission signature [11]. Physisorbed ethylene is not stable at the lowest crystal temperatures achieved with our apparatus ( $T = 110$  K) and is therefore populated only dynamically. Adsorption into the physisorbed state is not activated. Population of the  $\pi$ -bonded state on Ag(100) is inhibited for translational energies  $E_i < 0.35$  eV. It is, in contrast, non-activated on Ag(410): open steps therefore remove the adsorption barrier into such a little distorted state. This result is in qualitative agreement with *ab initio* calculations showing that ethylene adsorption on Ag(100) is stable only at adatoms [16, 17]. On Ag(410), initially, all molecules chemisorb. A less strongly bound moiety, metastable at the temperature of the experiment, appears only at higher coverage. Preliminary data on the  $C_2H_4$  interaction with Ag(210) were reported briefly in previous papers [14, 15] and are completed by the present, detailed, report on energy, angle and coverage dependence of the sticking probability.

## 2. Experimental details

The experimental set-up, consisting of a UHV chamber equipped with HREELS and usual surface science cleaning and testing tools coupled with a supersonic molecular beam, is described in detail elsewhere [18]. The sample is a 7 mm Ag single crystal oriented within  $0.25^\circ$  with the (210) direction. It is cleaned following the usual procedure of sputtering with 1 Ke Ne ions followed by annealing to 700 K. It can be cooled down to 110 K by fluxing liquid nitrogen through a cryostat. Surface order is checked by inspection of the low energy electron diffraction (LEED) pattern, while high resolution electron energy loss spectroscopy (HREELS) was employed in preliminary experiments to monitor surface cleanliness and to determine the nature of the adsorbed species and their desorption temperature. Dosing is performed by the supersonic molecular beam. The energy of the beam is controlled either by using pure ethylene or seeding it in He (3%  $C_2H_4$ ) and by heating the ceramic nozzle up to 870 K. The retarded reflector method of King and Wells (KW) [19] is employed to measure the sticking probability as a function of coverage after the beam flux has been carefully determined by use of a spinning rotor gauge (SRG) and a quadrupole mass spectrometer (QMS) not in line of sight with the beam. For these measurements the beam spot was collimated to a diameter of 2 mm for normal incidence onto the surface. The flux of the pure beam is measured directly by the SRG and reads  $0.094 \text{ ML s}^{-1}$ . For the seeded beam it is determined by comparing the QMS signal of the  $C_2H_4$  partial pressure rise with the one relative to the pure beam. The energy of the molecules is determined by time of flight. The full width at half maximum (FWHM) of the energy distribution is 20%. The scattering plane is aligned along the plane defined by the  $\langle 120 \rangle$  direction and the normal to the crystal. The angle of incidence  $\theta_i$  is defined with respect to the (210) crystal plane so that  $\theta_i = -26.5^\circ$  corresponds to the local normal of the (100) and  $\theta_i = +18.5^\circ$  to the one of the (110) nanofacets. (See the surface geometry in the inset of figure 1. The geometry of Ag(410) is also shown for comparison.) No measurements were performed for absolute values of  $\theta_i$  larger than  $60^\circ$  since the illuminated spot becomes then comparable to the diameter of the sample.

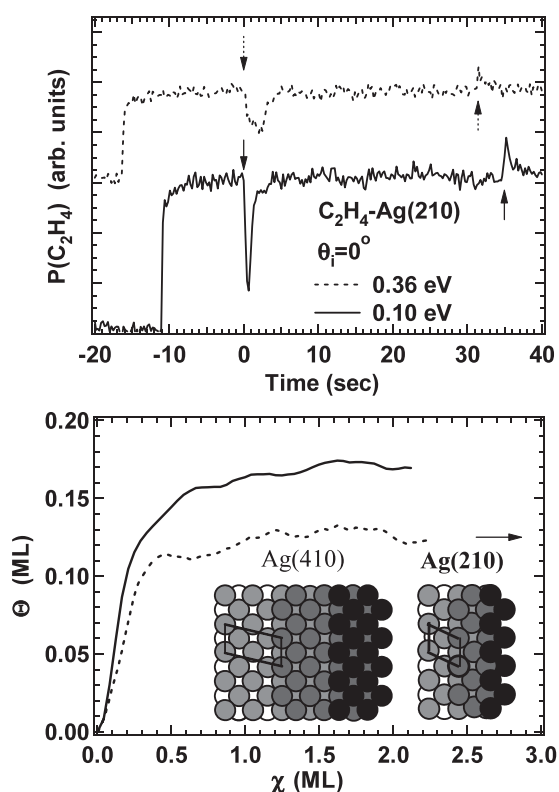


**Figure 1.** Upper panel: partial pressure of  $C_2H_4$  as a function of time in a typical KW experiment. The beam impinges normally onto the Ag(210) surface at  $T = 110$  K both for the pure (0.10 eV) and for the seeded beam (0.36 eV). Lower panel: coverage of ethylene versus exposure for the same experiments. The surface geometries of Ag(210) (right) and Ag(410) (left) are shown in the inset. The (210) surface consists of one atomic row wide (100) and (110) nanoterraces giving rise to open and reactive steps. On Ag(410), reported here for comparison, the (100) nanoterrace is three atomic rows wide.

### 3. Results and discussion

A typical KW experiment is shown in the upper panel of figure 1, where the QMS intensity at mass 26 (one of the main peaks of the ethylene cracking pattern) is reported as a function of time,  $t$ , for two beam energies and normal incidence. At  $t = 0$  an inert flag, initially intercepting the molecular beam in the crystal chamber, is removed. A drop in the  $C_2H_4$  partial pressure, due to adsorption at the surface, takes then place. The relative decrease is the sticking coefficient,  $S$ , and the missing area of the curve in the figure is directly proportional to the coverage. After some exposure time, the pressure approaches the initial level, indicating that the sticking probability has become lower than the experimental sensitivity of the KW method. If the beam is intercepted again by the flag (right arrow in figure 1), a transient increase in the ethylene signal is observed, corresponding to desorption of that part of the layer which is metastable at the temperature of the experiment. In the lower panel of figure 1 we report the dependence of surface coverage,  $\Theta$ , versus exposure,  $\chi$ , obtained from the traces of the upper panel. The coverage reached with the low energy beam after desorption of the metastable component is close to one eighth of a monolayer (ML) (see arrow), corresponding

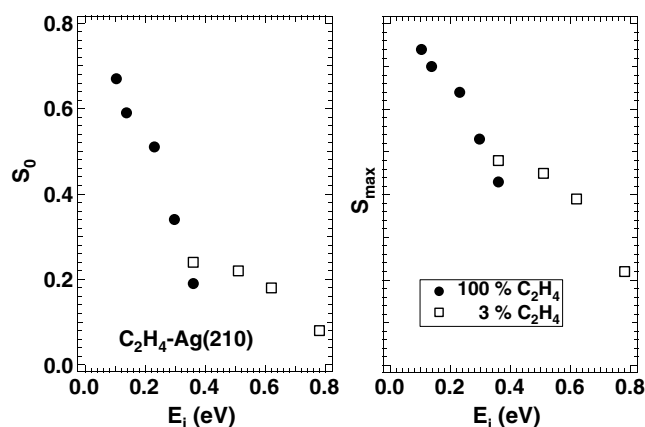


**Figure 2.** Initial,  $S_0$ , (left panel) and maximum,  $S_{\max}$ , (right panel) sticking probability versus translational energy for Ag(210) at  $T = 110$  K and for normal incidence onto the surface.

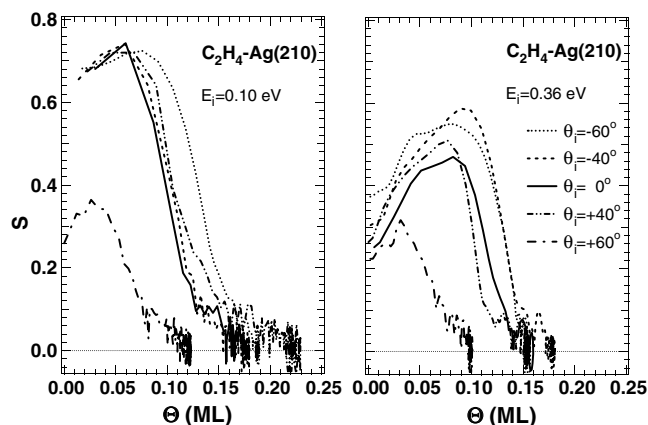


**Figure 3.** Coverage dependence of  $S$  parametric in the angle of incidence for the pure beam (left panel) and for the seeded beam (right panel).

to quarter occupancy of the step sites. A similar coverage is reached for the higher beam energy experiment.

In figure 2 we show the initial,  $S_0$ , and the maximum,  $S_{\max}$ , sticking probability as a function of translational energy,  $E_i$ , at a sample temperature  $T = 110$  K and at normal incidence<sup>1</sup>.  $S_0$  is obtained by fitting the linear part of the  $S(\Theta)$  curves (see figure 3) and taking its intercept with the left axis as  $S_0$ . This procedure is more accurate than the one, used in our previous report [15], of taking the relative drop in the partial pressure at the first experimental point after the molecular beam strikes the sample, since the sticking probability depends strongly on coverage. The  $S_0$  values so obtained are therefore slightly lower than reported in [15]. For  $C_2H_4/Ag(410)$ , where the slope of the  $S(\Theta)$  curve is smaller, both procedures yield the same value of  $S_0$  within experimental sensitivity. It is apparent that the sticking probability decreases with increasing translational energy, as expected for non-

<sup>1</sup> The dependence of  $S_{\max}$  was erroneously reported in [15] as the one of  $S_0$ . Little or no dependence of  $S_0$  on the internal energy is present, in agreement to the case of the adsorption on the Ag(410) surface.

activated systems and as observed also on Ag(100) and Ag(410). At  $E_i = 0.36$  eV, the experiment can be performed either with a hot nozzle, yielding a rotationally hot beam, or with a seeded beam with the nozzle at room temperature, yielding rotationally cold molecules. At variance with the case of  $C_2H_4$ -Ag(100), for which rotations inhibited physisorption [9], we find for the present system little or no difference both for  $S_0$  and for  $S_{max}$ . The different behaviour may be due either to the surface corrugation or to the stronger molecule-surface interaction leading to chemisorption. The situation is thus similar to  $C_2H_4$ /Ag(410), where rotational energy was found to inhibit adsorption at higher coverage only.

In figure 3 we show the coverage dependence of  $S$  for  $E_i = 0.10$  eV (left panel) and for  $E_i = 0.36$  eV (right panel) parametric in the angle of incidence,  $\theta_i$ . It is apparent that at the lower  $E_i$ ,  $S$  is nearly constant until a coverage of about 0.09 ML is reached. It decreases thereafter with  $\Theta$ , vanishing at about 0.18 ML. The coverage at which  $S$  vanishes (or, more correctly, becomes lower than the present experimental sensitivity of  $\approx 0.02$ ) is thereby nearly the same for all angles, except for grazing incidence on the (100) nanofacets ( $\theta_i = +60^\circ$ ). At larger  $E_i$ ,  $S$  increases linearly with coverage up to 0.10 ML, and decreases thereafter, vanishing between 0.13 and 0.18 ML. The final coverage, reached after desorption of the metastable molecules, is nearly angle independent (except again for  $\theta_i = +60^\circ$ , corresponding to grazing incidence on the (100) nanofaces).

The initial increase of  $S_0$  is due to the so-called adsorbate-assisted adsorption phenomenon [20, 21]. For a non-activated system, the higher the amount of energy the molecule loses in its collision with the surface, the higher is the sticking probability. Such energy transfer is more efficient when the impinging molecule collides with a previously adsorbed one than when it collides with a silver atom, because of the perfect mass matching.

When the coverage of 0.12 ML is reached no further molecules can adsorb stably at 110 K. This final coverage is the same as that found on Ag(410), even if the density of steps is twice as large. For that system, *ab initio* calculations by Kokalj *et al* [16] found that the stable adsorption site of  $C_2H_4$  involves the least coordinated Ag atoms, these being on the (100) terrace close to the step. The saturation coverage on Ag(410) indicates therefore that only non-neighbouring step sites can be populated by admolecules. In the case of  $C_2H_4$ /Ag(210), the distance to the nearest adsorption site on the neighbouring row is, however, comparable to the one of the next site on the same row and is therefore destabilized, too. Consistently only every second step is thus covered with ethylene. No  $(2 \times 2)$  superlattice was however observed with LEED.

In figure 4,  $S$  is plotted as a function of the angle of incidence for different coverage. The data points are obtained by analysing  $S(\Theta)$  curves similar to those reported in figure 3. It is apparent that  $S_0$  depends little on  $\theta_i$ , exhibiting a smooth decrease with increasing  $\theta_i$ . For  $E_i = 0.10$  eV it drops however at  $\theta_i = +60^\circ$ , corresponding to grazing incidence on the (100) nanofacets (we recall that positive values of  $\theta_i$  correspond to incidence with the momentum vector pointing against the (110) nanoterraces). This effect becomes more prominent at larger coverage, where  $S$  decreases at large  $\theta_i$  also at higher  $E_i$  and already for smaller angles. At  $E_i = 0.10$  eV a shallow minimum builds around normal incidence for  $\Theta > 0.09$  ML, which becomes more evident with increasing coverage. At 0.36 eV  $S$  decreases, in contrast, smoothly towards positive angles, the effect being larger at large  $\Theta$ .

The absence of an angle dependence of  $S_0$  is explained by the effectiveness of steering which forces the incoming molecules towards the adsorption site: a similar effect is indeed found for Ag(410) and is confirmed by trajectory simulations [22]. The effect is reduced at higher coverage, indicating that steering becomes less effective. We suggest that this is due to the decrease of the adsorption energy caused by the repulsive interactions between adsorbed molecules [23]. Indeed when steering is less efficient a minimum close to normal incidence is

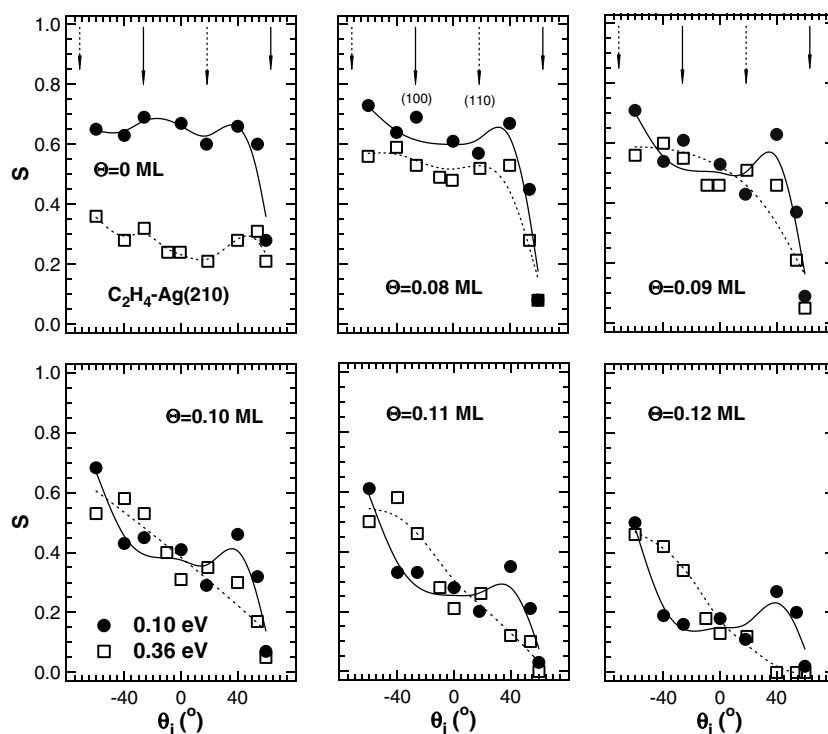


**Figure 4.** Angle dependence of the sticking probability for different coverages. The curves are guides to the eye. The arrows indicate the angles corresponding to incidence normal (long) and parallel (short) to (100) (continuous curve) and (110) (dashed curve) nanofacets.

expected, since molecules impinging along this direction have to dissipate a larger amount of energy in order to get trapped.

The decrease of  $S$  with increasing  $\theta_i$  at high coverage and large  $E_i$  takes place also for  $C_2H_4/Ag(410)$ . For that system we show that the effect is more important for rotationally cold beams [24]. This behaviour is thus linked to the compensation of steering, to rotational versus translational energy conversion, and to the energy transfer to the substrate.

Both  $S$  and the final attained coverage decrease eventually at large positive angles, i.e. for grazing incidence on the (100) nanoterraces (shadowing occurs for  $\theta_i > 64^\circ$ ). This effect reminds us of the similar drop observed for  $C_2H_4/Ag(410)$  when the (110) nanoterraces become shadowed, implying an enhanced reflection probability at grazing incidence on either of the nanoterraces building up the vicinal surface. This behaviour is counterintuitive, since the sticking probability should increase when less normal momentum needs to be dissipated. On an atomically stepped surface, however, the trapped molecules may be projected back into the vacuum when they reach the end of the nanoterrace if they have not dissipated enough parallel momentum. Interestingly, the effect becomes larger and more anisotropic at non-zero coverage, where the sticking probability is lowest for molecules impinging at grazing angle to the  $\langle 100 \rangle$  nanofacet. We believe this to be due again to the relatively small momentum transfer of the molecule upon colliding with an Ag atom, and to the stopping power of the ethylene admolecules, whose adsorption site is at the (100) side of the step according to theory [16]. Molecules impinging at grazing angle to the  $\langle 110 \rangle$  nanofacet will therefore have a larger chance to hit against already chemisorbed molecules and thus be stopped more efficiently.

The adsorbate assisted adsorption phenomenon is indeed weaker for positive  $\theta_i$ , as can be seen from the  $S(\Theta)$  curves in figure 3. Molecules impinging from positive angles and not hitting admolecules at the first strike will move along the surface towards the (110) side of the step where no further admolecules are present. In contrast, the molecules impinging at negative angles and not colliding directly against admolecules will eventually move towards the (100) nanofacet where the admolecules sit, and thus have a chance of hitting them and losing energy.

#### 4. Conclusions

In conclusion we have investigated ethylene adsorption on Ag(210) and compared the results with previous measurements on Ag(100) and Ag(410). The main findings can be summarized as follows.

- (1) The layer forming when dosing at 110 K consists of a stable part due to chemisorbed  $\pi$ -bonded molecules and of a metastable part of molecules desorbing within seconds at the end of the dose.
- (2) The initial sticking probability decreases with increasing translational energy as is the case for  $C_2H_4/Ag(410)$  and for  $C_2H_4/Ag(100)$ . The barrier to adsorption, preventing a stable layer from forming at low  $T$  on Ag(100) when dosing at low translational energy, is removed in the presence of the steps as is also the case for  $C_2H_4/Ag(410)$ .
- (3) The initial sticking probability shows little or no angle dependence as long as the incidence direction is not grazing onto the (100) nanofacet. The result is explained by the occurrence of steering of the incoming molecules towards the active site at the step, as is also the case for Ag(410).
- (4) At high coverage the angle dependence of  $S$  is more complex, exhibiting a shallow minimum around normal incidence for the pure beam and a smooth decrease with  $\theta_i$  for the seeded beam. The effect is due to the decrease of the adsorption energy with coverage, which makes steering less effective. The decrease of  $S$  for grazing angles on the (100) nanofacets is probably due to an enhanced probability of being reflected back into the vacuum.
- (5) The maximum coverage of chemisorbed ethylene is the same as for Ag(410), even if the density of steps is twice as large.

#### References

- [1] Somorjai G A 1994 *Surf. Sci.* **299/300** 849
- [2] Goodman D W 1994 *Surf. Sci.* **299/300** 837
- [3] Madix R J and Roberts J T 1994 *The Problem of Heterogenously Catalyzed Partial Oxidation: Model Studies on Single Crystal Surfaces* ed R J Madix (Heidelberg: Springer) chapter 1 (Surface Reactions)
- [4] Backx C, de Groot C P M and Biloen P 1980 *Appl. Surf. Sci.* **6** 256
- [5] Ertl G 2000 *Adv. Catal.* **45** 1
- [6] Van Santen R A and Kuipers H P C 1987 *Adv. Catal.* **35** 265
- [7] Campbell C T 1985 *Surf. Sci.* **157** 43
- [8] Bocquet M-L, Michaelides A, Loffreda D, Sautet P, Alavi A and King D A 2003 *J. Am. Chem. Soc.* **125** 5620
- [9] Vattuone L, Valbusa U and Rocca M 1999 *Phys. Rev. Lett.* **82** 4878
- [10] Vattuone L, Savio L, Rocca M and Valbusa U 2000 *Chem. Phys. Lett.* **331** 177
- [11] Vattuone L, Savio L, Rocca M, Rumiz L, Baraldi A, Lizzit S and Comelli G 2002 *Phys. Rev. B* **66** 85403
- [12] Rocca M, Savio L and Vattuone L 2002 *Surf. Sci.* **502/503** 331
- [13] Savio L, Vattuone L and Rocca M 2003 *J. Electron Spectrosc. Relat. Phenom.* **129** 157
- [14] Vattuone L, Savio L and Rocca M 2003 *Int. J. Mod. Phys. B* **17** 2497
- [15] Vattuone L, Savio L and Rocca M 2003 *The Chemical Physics of Solid Surfaces* vol 11, ed D P Woodruff (Amsterdam: Elsevier)



- 
- [16] Kokalj A, Dal Corso A, de Gironcoli S and Baroni S 2002 *Surf. Sci.* **507–510** 62
  - [17] Kokalj A, Dal Corso A, de Gironcoli S and Baroni S 2002 *J. Phys. Chem. B* **106** 9839
  - [18] Rocca M, Valbusa U, Gussoni A, Maloberti G and Racca L 1991 *Rev. Sci. Instrum.* **62** 2171
  - [19] King D A and Wells M G 1972 *Surf. Sci.* **29** 454
  - [20] Arumainayagam C R, McMaster M C and Madix R J 1991 *J. Phys. Chem.* **95** 2461
  - [21] Siddiqui H R, Chen P J, Guo X and Yates J T Jr 1990 *J. Chem. Phys.* **92** 7690
  - [22] Savio L, Vattuone L, Rocca M, Corriol C, Darling G R and Holloway S 2003 *Chem. Phys. Lett.* **382** 605
  - [23] Vattuone L, Yeo Y Y and King D A 1996 *Catal. Lett.* **41** 919
  - [24] Vattuone L, Savio L and Rocca M 2004 in preparation